STRANGENESS PRODUCTION IN HEAVY-ION COLLISIONS AT INTERMEDIATE ENERGIES REVISITED WITH PIONS*

Krzysztof Wiśniewski

for the FOPI Collaboration

Institute of Experimental Physics, University of Warsaw
Hoża 69, 00-681 Warsaw, Poland

(Received January 14, 2010)

In this contribution, we give a short summary of experimental results on the production of strangeness, especially of charged kaons, in heavy-ion collisions at intermediate energies. In particular, we discuss the possible interpretation of these results, which suggests that properties of hadrons are modified in a dense nuclear matter. We point out to problems connected to this interpretation, for example, unknown cross-sections of the underlying elementary process. We discuss in detail an experiment that aimed at measuring these cross-sections at the normal nuclear matter density. We present experimental results on the production of neutral kaons in collisions of pions at 1.15 GeV/c incident momentum with C, Al, Cu, Sn, Pb nuclei. We focus on the inclusive production cross-sections and the phase-space distributions of the produced K^0 mesons, which both shed more light on the problematic issues and point out to the modifications of the elementary reaction amplitudes as well as of the KN potentials in the baryonic matter at the normal nuclear matter density.

PACS numbers: 25.80.Hp, 24.80.+y

1. Introduction

Production of strange particles in heavy-ion collisions has been studied in order to learn, among others, about the nuclear equation of state [1] and about modifications of properties of hadrons that take place in a dense hadronic matter [2]. At intermediate energies, close to the elementary production threshold, strangeness can be produced, in the first-chance nucleon–nucleon collisions: $NN \to KY$ or $NN \to K\bar{K}NN$, where K, $\bar{K}$ and Y stand

* Presented at the XXXI Mazurian Lakes Conference on Physics, Piaski, Poland, August 30–September 6, 2009.

for a kaon, an antikaon and an appropriate hyperon, respectively. In addition, when the nuclear matter is compressed and heated, excited states of nucleons are populated as well, which opens new production channels involving Δ's and pions: $\Delta N \to KY$, $\pi N \to KY$. Most of the strangeness is produced, in the first stage of such collisions, whereas in later stages, the energy density of the matter is not anymore sufficiently high for a production of a pair of strange–antistrange quarks.

Because of the strangeness exchange reactions: $\bar{K}N \leftrightarrow \pi Y$, yields of antikaons and hyperons vary during later stages of heavy-ion collisions, before the chemical freezout takes place. Indeed, results of transport model calculations show, for example, that a substantial fraction of $\bar{K}$ meson yield that is eventually measured may originate from these processes [3]. Contrary, kaons (K^+, K^0) can be hardly reabsorbed after the production, because in this case only the charge exchange reactions can take place: $K^+n \leftrightarrow K^0p$. Therefore, especially kaons are considered to be a good probe to study the properties of the dense and hot nuclear matter that is created in heavy-ion collisions at intermediate energies [4].

Depending on the stiffness of the nuclear equation of state, the available energy is appropriately partitioned between the compressional energy and the kinetic energies of participating nucleons. This influences the production of particles, for example kaons, originating from the hot and dense zone of the collision. Comparison of the production probabilities of K^+ mesons in C+C and Au+Au collisions at energies below and close to the elementary threshold, measured by the KaoS Collaboration, show that the inclusive production cross-section drops less steeply with decreasing beam energy in the case of the heavy system [5]. This could not happen if the nuclear matter were very hard to compress. Indeed, results of the QMD-transport-model calculations reproduce the trend observed in the data when the adopted parameterization corresponds to compressibility parameter of 200 MeV [6]. Such soft equation of state leads to higher compression in the case of the Au+Au system, in which secondary production channels open and dominate the kaon production, especially below the elementary NN threshold.

The anticipated change of the kaon mass [7], which, according to theoretical predictions rise with the increasing matter density, acts on the kaon production in the opposite way, *i.e.* the more the matter is compressed, the smaller the yield of produced kaons is expected. There are several experimental results that point towards scenario of in-medium modifications of hadron masses, in particular the rise of the effective kaon mass and the drop of the effective mass of the antikaon, due to the vector and scalar parts of the kaon–nucleon interactions.

It was, for example, observed that phase-space distributions of K^+ and K^- mesons produced in Ni+Ni collisions at 1.9 A GeV beam energy are different, *i.e.*, the distribution of the K^- mesons is more compact than that of the K^+ mesons [8]. According to the results of the BUU transport-model calculations, this could not be explained by simple kinematical effects, in particular by differences at the time of the production in elementary, nucleon–nucleon collisions, which in the case of K^- mesons involves three particles in the exit channel. The experimental data could be reproduced by the model only when the in-medium modifications of kaons were taken into account.

The flow of the K^+ mesons was measured in Ru+Ru collisions at 1.7 A GeV beam energy. On average, *i.e.*, in terms of the $v1 = \langle \cos(\phi) \rangle$ component (where ϕ stands for the azimuthal angle with respect to the reaction plane), K^+ mesons showed zero-flow signal both in central as well as in peripheral collisions, whereas differentially, *i.e.*, in terms of the $v2$ component, anti-flow signal was observed for kaons of low transverse momenta in peripheral reactions [9]. Both observations were nicely reproduced by the BUU transport-model calculations when additional repulsion of the medium (leading to the rise of the effective kaon mass) was taken into account. Similar conclusions were drawn when the squeeze-out, *i.e.*, preferential out-of-plane emission of K^+ mesons was measured in Au+Au collisions at 1.0 A GeV energy [10]. Results of the BUU-model calculations agreed with the experimental data, when additional repulsion of the mean-field potential, due to the surrounding medium was included in the calculations.

One encounters several problems when one tries to draw conclusions about the in-medium effects on kaons by comparing experimental observation to results of model calculations. Commonly used BUU- or QMD-like transport codes require more input than only whether or not and to which extent these effects are to be accounted for. One of the key ingredients of such calculations are the considered production channels. It has been recently realized that, for example, a substantial fraction of K^- mesons (up to 20%) measured in nucleus–nucleus collisions close to the elementary production threshold may steam from decays of the $\phi(1020)$ mesons [11], which have till now not been thought to influence the final K^- meson yields and have not been considered as an important component in most transport codes.

Usually considered production channels have to be examined with much conscious as well. Thanks to the results of model calculations, one anticipates that two-step processes, in which a pion produced in NN collision hits subsequently a second nucleon: $\pi N \rightarrow KY$, are among the dominating ones for kaon production in heavy-ion collisions at energies close to the elementary-reaction threshold [12]. Cross-sections of such processes has been measured in broad energy range and are very well known in vacuum. How-

ever, it has been suggested recently that, due to the in-medium modifications of the involved particles, there should be a dramatic change of the thresholds and the cross-sections of the elementary $\pi N \to YK$ processes if they take place in dense nuclear matter [13]. Unfortunately, an attempt to evidence this effect in proton–nucleus experiments has not been successful till now [14]. Thus, the conjecture that was essential to many previous studies concerned with the strangeness production in heavy-ion collisions at near-threshold energies still awaits its experimental confirmation. An appropriate measurement of these effects would thus be of a great importance for understanding and proper interpretation of previous experimental results on the strangeness production in heavy-ion collisions.

In order to achieve this goal, one may try to study collisions of pions with nuclei and observe production of strangeness from reactions on individual nucleons that are surrounded by medium of density ρ_0. First studies of the associated $\Lambda\, K^0$ production from πA reactions date to the early sixties. The reactions at energies near the threshold of the elementary process were studied at AGS at BNL with bubble chamber and spark chamber detectors [15]. The main limitations of those older studies were low statistics (from a few up to a few hundred counts), special triggering system (rejecting the low momentum particles), and a wide spread of the incident pion momenta (of a few hundred of MeV/c). Because of them, the energy dependence of the production cross-sections cannot be extracted from those experimental results with a satisfactory accuracy. In contrast, the modern hyper-nuclei experiments are truly high statistics and very good precision measurements. In fact, those capable of measuring the quasi-free Λ production, like the SKS spectrometer at KEK [16], could provide precise information about the production cross-sections. However, the different physics scope and the used apparatus limit such measurements to relatively high momenta ($p_K >$ 600 MeV/c) and to forward angles ($\Theta_{\rm lab} < 15^\circ$), whereas it is well known that, for example, the angular distributions of Λ and K^0 mesons from the $\pi^- p \to \Lambda\, K^0$ reaction is highly non isotropic. Moreover, predictions are made that these distributions should change appreciably when the process takes place in the nuclear medium [13].

In order to overcome these limitations, a new experiment was design with the apparatus that almost ideally fulfills all the requirements of a proper, precision measurement (see below). The associated strangeness production by negative pions of 1.15 GeV/c momenta on various nuclear targets was studied using the FOPI spectrometer on the SIS accelerator at GSI. One has to keep in mind that in general, an obvious disadvantage of such an experiment is that pions cannot penetrate too deeply inside nuclei, due to very large absorption cross-section to form, for example, higher nucleon-resonances. On the other hand, the conditions reached in pion–nucleus collisions are better defined than those of heavy-ion reactions. The role of the secondary processes can be investigated more directly than even in pA studies.

2. Experiment

The π^- — beam was delivered by the SIS accelerator at GSI. On average, about 10^{10} pions were produced by the Carbon beam of 2.0 A GeV energy on the primary Beryllium target. The secondary beam was transported down the 89 meters long beam-line to the FOPI spectrometer, where pions hit five different targets: C, Al, Cu, Sn, and Pb, with thicknesses of 1.87, 1.56, 4.41, 2.83 and 5.76 g/cm^2, respectively. The beam optics was adjusted in the way that on average about 3000 π^-/s with a mean momentum of 1.15 GeV/c and a momentum dispersion of about 0.5% were registered at the place of the experiment. The chosen beam momentum corresponded to an available energy $\sqrt{s}$ of about 1.75 GeV in the system of π^- mesons colliding with nucleons at rest.

The FOPI spectrometer is a modular system of high granularity and large geometrical acceptance [17]. Two drift chambers (CDC and Helitron) and two corresponding time-of-flight walls (Barrel and Plastic Wall) are the main components of the setup. The setup, shown schematically in Fig. 1, is placed inside a superconducting solenoid magnet, which delivers magnetic field of about 0.6 T. The spectrometer is capable of simultaneous measur-

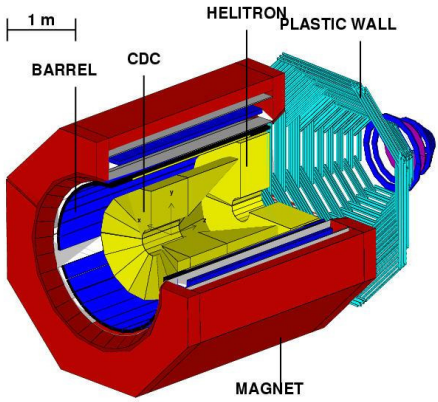


Fig. 1. Schematic view of the FOPI experimental setup.

ing large fraction of all the charged particles produced in reactions on the target. Identification of the reaction products, with respect to their charges and masses, is based on the measurement of the specific energy loss and the curvature of tracks in the drift chambers and the velocity deduced from the time-of-flight, measured in the plastic scintillators. Neutral particles normally escape the detector without being identified, unless they are short-lived and decay inside the setup into charged secondaries. In such case they can be identified by reconstruction of the invariant mass of their decay products. The results presented in this contribution were restricted to K^0_S

mesons reconstructed via their decays into $(\pi^-,\ \pi^+)$ pairs within the geometrical acceptance of the Central Drift Chamber, *i.e.*, in the range of polar angles in the laboratory frame $25^\circ < \theta < 150^\circ$.

Altogether about 25 million events were registered under a minimum-bias trigger condition, *i.e.* in case that at least a single charged particle was detected inside the CDC. The position of the primary interaction point was reconstructed with the help of two silicon micro-strip detector stations, each consisting of two single sided detectors ($3.2 \times 3.2\text{cm}^2$ area, 300 μm in thickness and with 50 μm pitch size) and placed 94 cm and 224 cm upstream from the target.

In the upper plot in Fig. 2 the invariant mass distribution of (π^-, π^+) pairs registered in $\pi^- + \text{Pb}$ reactions is shown. The lower plot of this figure shows the distribution after subtracting the background, the shape of which was estimated by the event mixing-method. In order to reduce the combinatorial background below the K^0_S peak, tracks of positive and negative pions, that entered in the analysis, were carefully chosen by imposing selection criteria on the parameters of the tracks. Reconstructed transverse momenta of the considered particles, $p_{\text{t}}(\pi^-, \pi^+)$, were grater than 80 MeV/c. Assigned masses of particles, $\text{m}(\pi^-, \pi^+)$, were within the 0.05–0.6 GeV/c^2 interval. Only tracks which did not originate from the primary interaction point were

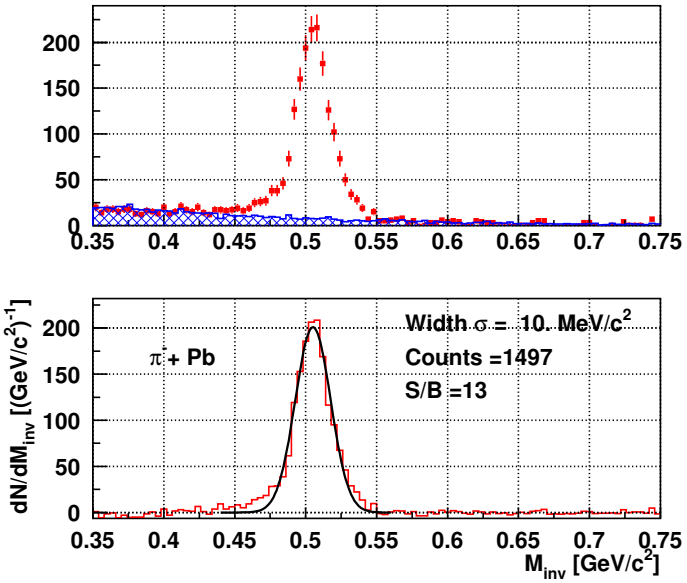


Fig. 2. Upper plot: the invariant mass distribution of selected (π^-, π^+) pairs registered in $\pi^- + \text{Pb}$ reactions and the corresponding combinatorial background. Lower plot: The invariant mass distribution from the upper plot after the background subtraction, with the Gaussian fit to the peak corresponding to K^0_S meson decays into (π^-, π^+) pairs.

selected by requiring that their distances of the closest approach to the primary vertex, $|d_0(\pi^-, \pi^+)|$, were grater than 1.5 cm. The differences between the azimuthal angles of reconstructed secondary vertices and momenta of kaons, $|\Delta\phi|$, were smaller than 30°.

After subtraction of the background, the distributions of invariant masses of (π^-, π^+) pairs are fitted with a Gaussian function around the nominal K^0_S meson mass, and the total number of reconstructed K^0_S mesons is estimated by integrating the result of the fit in the interval of $\pm\ 2\sigma$ around the centroid of the fited peak. This leads to an estimate of the total number of K^0_S meson reconstructed in the case of each target, which are given in Table I.

TABLE I

Statistics of K^0_S mesons accumulated on various targets.

Target	C	Al	Cu	SN	Pb
K^0_S reconstructed	1303	126	280	140	1495

3. Production cross-sections

In order to estimate the K^0 production cross-sections, the number of reconstructed K^0_S mesons is corrected in order to account for the branching ratio into $K^0_{S/L}$, the normalization to the number of beam particles and the target thickness, as well as the geometrical acceptance and the detection efficiency of the apparatus. The latter was estimated with the help of the GEANT simulation package, which aims at the realistic description of the FOPI detector response-function, including, in the case of the CDC, the production of the primary ionization, the subsequent drift and collection of electrons on the sense wires, the digitization of the collected charge, and the efficiency of the track-reconstruction algorithms. It should be also stressed, that given that the K^0 meson phase-space distribution were similar to the one predicted by the detailed transport-model calculations, about 85% of the production cross-section can be reconstructed in the geometrical acceptance of the experiment, due to its large geometrical coverage.

The dependence of the K^0 inclusive production cross-section on the mass of the target nucleus, A, is shown in Fig. 3 with error bars attached to the points representing the statistical uncertainties and boxes representing the systematic errors due to the details of the analysis of the experimental data. The dependance is fitted with a power law function: $\sigma(\pi^- + A \rightarrow K^0 + X) = \sigma_{\text{eff}}\, A^b$. The result of the fit yields $\sigma_{\text{eff}} = 0.87 \pm 0.13$ mb and $b = 0.67 \pm 0.03$, with a statistical error of $\chi^2/ndf = 0.9/3$. This A-dependence suggests that, in the studied reactions, kaons are produced at the surface of the nucleus.

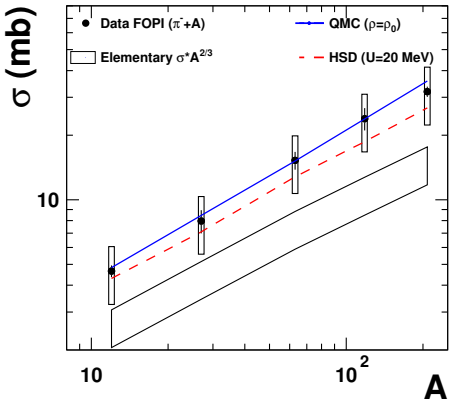


Fig. 3. The K^0 inclusive production cross-section (points) as a function of the mass number of the target nucleus. Experimental data are compared to predictions of the HSD transport model (dashed line) and to results of the simple calculations that adopt elementary cross-sections predicted by the QMC model (solid line).The large box area corresponds to the results of the calculation in which production of kaons takes place on the surface of the nucleus with the elementary production cross-section.

In Fig. 3, the measured inclusive cross-sections are compared to results of simple calculations based on the assumption that the production of kaons takes place only on the surface of target nuclei, depicted by box-area, which corresponds to about 20% of the experimental uncertainties. The known cross-sections of all the possible elementary processes in vacuum: $\pi^- + p \to K^0\ \Sigma^0$, $\pi^- + p \to K^0\ \Lambda$ and $\pi^- + n \to \Sigma^-\ K^0$ were weighted with the relative neutron (N/A) and proton (Z/A) contents of the target nuclei and multiplied by $A^{2/3}$, in order to account of the effective number of nucleons on the nucleus surface. One sees that the results of the calculations does not match the experimental observations, and underpredicts the measured cross-sections by about a factor of 2, which indicates that some essential part of the production process is missing. Enhanced production of strangeness on nuclear targets, with respect to the reactions in vacuum, especially at sub-threshold energies, is often explained by 'trivial' medium effects, *e.g.*, multi-step processes and/or Fermi momentum [18]. However, in the present case, both the elementary $\pi^- + N \to KY$ as well as $\Delta + N \to KYN$ production cross-sections are also on average significantly smaller than the extracted $\sigma_{\rm eff} = 0.87 \pm 0.13$ mb, even when taking the full advantage of the Fermi momenta of nucleons inside the nuclei. On the other

hand, the experimental results are reproduced well by the QMC model when modifications of the cross-sections of the elementary reactions at $\rho = \rho_0$ are taken into account [13] (solid line in Fig. 3), and the results of the calculations are scaled by the sizes of the target nuclei as described above. This may suggest that, despite the strong pion absorption on the surface of nuclei, the density at which kaons are produced is on average significant, which, in fact, is also confirmed by the results of the detailed Hadron-String-Dynamics (HSD) transport-model calculations [19].

The results of the HSD transport model calculations can be compared directly to the measured inclusive production cross-sections, which is shown by the dashed line in Fig. 3. While in the QMC model the K^0 production cross-section is changed due to the modifications of masses of the mesons, baryons and of the intermediate resonances, HSD parametrizes the medium effect by an effective, proportional to the local density, repulsive potential for kaons only. No sensitivity to such a KN potential is found within the HSD model for the inclusive K^0 production cross-section, *i.e.* the calculation without the KN potential predict a cross-section that is larger by only 3% than the one shown in Fig. 3. A measurable sensitivity is expected only for kaons that, after production, experience the influence of the medium for a long time. An analysis of the momentum distributions of K^0_S produced in $\pi^- + C$ and $\pi^- + \mathrm{Pb}$ reactions shows that most of them have rather large momenta, of more than 400 MeV/c, with respect to the target nucleus at rest. Consequently the average kaon kinetic energies are large compared to the expected size of the KN potential and, in order to achieve a sensitivity to this quantity, one has to focus on kaons with low momenta.

4. Phase-space distributions

One can learn more about the KN potential by comparing the phase-space distributions of kaons produced on heavy and light targets [20] in particular at low momenta. Such a comparison is made in Fig. 4 in terms of the yields-ratios of K^0_S produced on the Pb and the C targets as a function of the kaon momenta. This method implies reduction of systematic errors due to the cancellation of apparatus and analysis effects (like the detection and reconstruction efficiencies). One can observe that at higher momenta, $p > 170$ MeV/c, the yield of K^0_S mesons produced on the Pb target falls down more steeply with increasing momenta of kaons as compared to the the one on the C target. However, at lower momenta this trend is reversed: up to $p \simeq 170$ MeV/c, the momentum spectrum is steeper in the case of the C than in the case of the Pb target. This gives rise to a characteristic maximum in the yields-ratio plotted in Fig. 4. The observed behaviour can be understood if one thinks of an additional acceleration of K^0 mesons of low momenta due to the repulsive in-medium KN nucleon potential. Results of the transport model calculations show that in the case of the Pb target

on average kaons are produced in the medium which has a higher density. Therefore, one expects that the effect of the acceleration is bigger in this case as well.

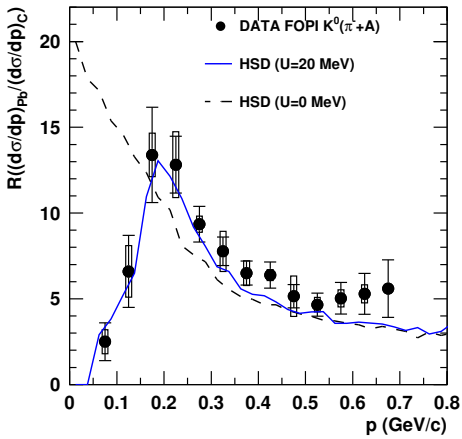


Fig. 4. The yields-ratio of K^0_S mesons produced by pions on heavy and light targets as a function of kaon momenta. The error bars correspond to the statistical uncertainty while the boxes attached to the points represent the systematic errors estimated by applying different methods of analysis. The data is compared to the results of the HSD model with different strength of the KN potential, depicted by solid and dashed lines.

In Fig. 4, the measured yields-ratio is compared to the results of the HSD-model calculations [19]. In order to allow for a direct comparison, the output of the calculations was corrected due to the geometrical acceptance of the experiment and the detection efficiencies. Two versions of the model are shown in Fig. 4: *(i)* including a K^0N potential of 20 MeV at ρ_0 (solid line) and *(ii)* without the K^0N potential (dashed line). Both versions take into account the K^0 rescattering after the production as well. The version of the model including a 20 MeV K^0N potential at ρ_0 (with a linear dependence of the potential on the nuclear density ρ) reproduces the measurements over the full momentum range, while the version of the model without a K^0N potential misses the trend in the data at low momenta completely.

The result presented in this work has a clear advantage over a similar analysis performed by the ANKE Collaboration on the K^+ meson production by protons of 2.3 GeV energy on Au and C targets [20], which also indicated the strength of the K^+N potential of the order of 20 MeV at ρ_0. In the present work, the strength of the repulsive KN interaction is extracted more directly, because the propagation of neutral kaons is not affected by the (additional) repulsive Coulomb interaction, which in the case of Au nuclei is as large as 15 MeV. In order to determine the accuracy with

which the effective K^0N potential of 20 ± 5 MeV was inferred from the comparison of the data to HSD-model, detailed χ^2 analyses of differences between the results of the model and the data were performed. This precision is presently limited only by statistics, which can be improved by new measurements, after the intensity upgrade of the SIS18 accelerator.

5. Summary

In summary, K^0 meson inclusive production cross-sections in reactions of π^- mesons at 1.15 GeV/c momentum ($\sqrt{s} \simeq 1.75$ GeV) with different targets: C, Al, Cu, Sn, and Pb were measured. The results were compared to predictions of the QMC model, and could be explained if possible changes of reaction amplitudes of the underlying elementary processes were assumed. The yields-ratio of K^0_S mesons produced on heavy (Pb) and light (C) nuclei was studied in detail a function of kaon momenta. Substantial suppression of the number of K^0_S mesons produced on heavy target was observed at low momenta. The observation could be reproduced by the HSD transport model calculations which includes the in-medium repulsive KN potential of 20 ± 5 MeV at $\rho = \rho_0$.

This work was supported by the Polish Ministry of Science and Higher Education under the Grant No. DFG/34/2007.

REFERENCES

[1] J. Aichelin, C.M. Ko, *Phys. Rev. Lett.* **55**, 2661 (1985); S.W. Huang *et al.*, *Phys. Lett.* **B298**, 41 (1993); C. Hartnack *et al.*, *Nucl. Phys.* **A580**, 643 (1994); G.Q. Li, C.M. Ko, *Phys. Lett.* **B349**, 405 (1995); B.-A. Li, *Phys. Rev.* **C50**, 2144 (1994).

[2] D.B. Kaplan, A.E. Nalson, *Phys. Lett.* **B175**, 57 (1986); T. Waas *et al.*, *Phys. Lett.* **B379**, 34 (1996).

[3] Ch. Hartnack, H. Oeschler, J. Aichelin, *Phys. Rev. Lett.* **90**, 102302 (2003).

[4] C. Fuchs, *Prog. Part. Nucl. Phys.* **56**, 1 (2006).

[5] C. Sturm *et al.*, *Phys. Rev. Lett.* **86**, 39 (2001).

[6] C. Fuchs, *Phys. Rev. Lett.* **86**, 1974 (2001).

[7] G.E. Brown *et al.*, *Nucl. Phys.* **A567**, 937 (1994); W. Weise, *Nucl. Phys.* **A610**, 35c (1996); G.Q. Li *et al.*, *Nucl. Phys.* **A625**, 372 (1997).

[8] K. Wisniewski *et al.*, *Eur. Phys. J.* **A9**, 515 (2000).

[9] P. Crochet *et al.*, *Phys. Lett.* **B486**, 6 (2000).

[10] Y. Shin *et al.*, *Phys. Rev. Lett.* **81**, 1576 (1998).

[11] A. Mangiarotti *et al.*, *Nucl. Phys.* **A714**, 89 (2003).

[12] E.L. Bratkovskaya, W. Cassing, U. Mosel, *Nucl. Phys.* **A622**, 593 (1997); C. Hartnack, J. Aichelin, *J. Phys. G* **28**, 1649 (2002).

[13] K. Tsushima, A. Sibirtsev, A.W. Thomas, *Phys. Rev.* **C62**, 064904 (2000).

[14] M. Büscher *et al.*, *Phys. Rev.* **C65**, 014603 (2002).

[15] Y.S. Kim *et al.*, *Phys. Rev.* **B140**, 1655 (1965); T. Bowen *et al.*, *Phys. Rev.* **119**, 2030 (1960).

[16] T. Fukuda *et al.*, *Nucl. Instrum. Methods* **A361**, 485 (1995).

[17] A. Gobbi [FOPI Collaboration], *Nucl. Instrum. Methods* **A324**, 156 (1993); J. Ritman [FOPI Collaboration], *Nucl. Phys. Proc. Suppl.* **44**, 708 (1995).

[18] V.P. Koptev *et al.*, *Sov. Phys. JETP* **67**, 2177 (1988); W. Cassing *et al.*, *Phys. Lett.* **B238**, 25 (1990); V.P. Koptev *et al.*, *Phys. Rev. Lett.* **87**, 022301 (2001).

[19] W. Cassing *et al.*, *Phys. Rep.* **308**, 65 (1999); W. Cassing *et al.*, *Nucl. Phys.* **A614**, 415 (1997).

[20] M. Buescher *et al.*, *Eur. Phys. J.* **A22**, 301 (2004).